

Direct evidence of core excitation in the giant resonance through the $(e, e'n)$ reaction

T. Saito,* K. Yoshida,† M. Oikawa,‡ Y. Suga,§ and K. Kino¶

Laboratory of Nuclear Science, Tohoku University, Mikamine, Taihaku-ku, Sendai 982-0826, Japan

T. Nakagawa** and T. Tohei

Department of Physics, Tohoku University, Aramaki, Aoba-ku, Sendai 980-8578, Japan

K. Abe

Department of Engineering, Tohoku University, Aramaki, Aoba-ku, Sendai 980-8579, Japan

H. Ueno

Department of Physics, Yamagata University, Kojirakawa, Yamagata 990-8560, Japan

(Received 22 December 2004; published 23 June 2005)

Angular correlations and cross sections for the $^{40}\text{Ca}(e, e'n)^{39}\text{Ca}$ reaction have been measured in the continuum above the giant resonance. A comparison of the missing energy spectra between the peak and the tail regions of the giant resonance indicates that neutron emission in the peak region leads to populating the ground and first excited states, whereas emission in the tail region leads to populating excited states at an energy about 4.5 MeV higher. The latter seems to be because of the $2s_{1/2}$ and $1d_{5/2}$ hole excitation, that is core excitation. The same tendency was observed in the $^{28}\text{Si}(e, e'n)^{27}\text{Si}$ reaction of the sd shell nuclei but it did not appear as clearly in the $^{12}\text{C}(e, e'n)^{11}\text{C}$ reaction of the $1p$ shell nuclei.

DOI: 10.1103/PhysRevC.71.064313

PACS number(s): 25.30.Dh, 24.30.Cz, 27.40.+z

The reaction mechanisms for the photon- or electron-nucleon emission reaction have been studied extensively. Most studies have been done in the giant dipole resonance (GDR) region, where the reaction mechanism is quite well understood. In the continuum just above the GDR, experimental data are rather scarce and the reaction mechanism is not clear.

Coincidence electron-scattering experiments such as $(e, e'p)$ and $(e, e'n)$ can provide new insight into nuclear structure and dynamics. The $(e, e'n)$ reaction is suitable for the study of the giant resonance since in this reaction the quasifree knockout (QFK) process is expected to be very small in contrast to the $(e, e'p)$ reaction.

In the previous study [1], angular correlations for the $^{12}\text{C}(e, e'p_0)$ [2] and $^{12}\text{C}(e, e'n_0)$ [1] reactions in the continuum above the GDR were compared with recent Hartree-Fock (HF) and random-phase approximation (RPA) predictions [2,3]. The HF approach corresponds to a QFK reaction mechanism and its predictions are uniquely determined by the single-particle

properties of the target nucleus. Conversely, the contribution from initial and final state correlations is accounted for through the RPA. From the comparison with these predictions, it was suggested that RPA correlations were crucial for the interpretation of the $(e, e'n_0)$ reaction in the continuum. The present article reports on measurements of the missing energy spectra and angular correlations for the $^{40}\text{Ca}(e, e'n)$ reaction in the continuum above the GDR and compares the results with those of $^{12}\text{C}(e, e'n)$ [1] and $^{28}\text{Si}(e, e'n)$ [4]. The giant resonances in ^{40}Ca and ^{48}Ca via the $(e, e'n)$ reaction have been measured previously [5,6].

The $^{40}\text{Ca}(e, e'n)$ experiment was performed using the continuous electron beam from the 150-MeV Tohoku University pulse stretcher ring [7]. A natural calcium target of thickness 95.2 mg/cm² was bombarded with electrons of energy 129 MeV. Scattered electrons were detected at $\theta_e = 30^\circ$ by a magnetic spectrometer that has a solid angle of 5 msr and a momentum resolution of 0.05% within the accepted momentum bite of 5.3%. Neutrons emitted from the target were measured using 10 NE213 liquid scintillator neutron detectors.

These were placed in the electron scattering plane at $\theta_n = 50^\circ$ to 270° at 20-degree intervals except for the angles between $\theta_n = 150^\circ$ and 210° . Each detector was placed 105 cm from the target allowing the neutron energy to be determined by the time-of-flight method. The neutron detectors were shielded with lead, paraffin, and concrete, and lead collimators were placed in front of 4-cm-thick bismuth plates to absorb scattered electrons and soft γ rays from the target. The neutron detectors were calibrated using γ rays from ^{22}Na , ^{137}Cs , ^{60}Co , and Am-Be sources. The Compton edge of the ^{137}Cs γ ray was utilized to set the detection threshold. The neutron efficiency for the detectors was determined using a ^{252}Cf source and an

*Present address: Faculty of Engineering, Tohoku Gakuin University, Chuo, Tagajo 985-8537, Japan.

†Present address: Toshiba Co. Shibaura, Minato-ku, Tokyo 105-0023, Japan.

‡Present address: 5th Research Center, Technical Research & Development Institute, Japan Defense Agency, Nagase, Yokosuka 239-0826, Japan.

§Present address: Hitachi Software Engineering Co., Nakase, Mihama-ku, Chiba 261-0023, Japan.

¶Present address: Research Center for Nuclear Physics, Osaka University, Ibaraki 567-0047, Japan.

**Present address: Tohoku Institute of Technology, Kasumi-cho, Taihaku-ku, Sendai 982-8577, Japan.

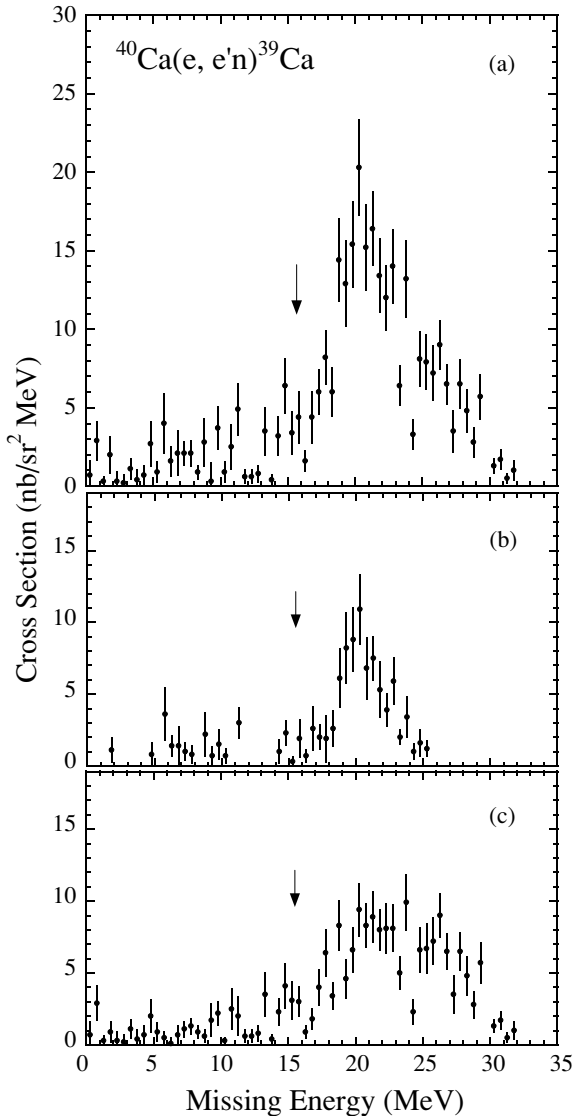


FIG. 1. Missing energy spectra for the $^{40}\text{Ca}(e, e'n)^{39}\text{Ca}$ reaction at $\theta_n = 70^\circ$ for the excitation energy range (a) $\omega = 28\text{--}35$ MeV, (b) $\omega = 28\text{--}30$ MeV, and (c) $\omega = 31\text{--}35$ MeV. Arrows indicate the position of the ground-state transitions.

analytical calculation code. The details of electronics, data acquisition, and detection efficiency are described elsewhere [8].

The missing energy spectrum for the $^{40}\text{Ca}(e, e'n)$ reaction at $\theta_n = 70^\circ$ for a range of excitation energy ω , between 28 and 35 MeV (hereafter this region above the giant resonance is called the tail region) is shown in Fig. 1(a). No strong ground-state transition was observed at 15.6 MeV, indicated by an arrow, but only a broad peak was observed around 20 MeV. Separate missing energy spectra for $\omega = 28\text{--}30$ and $31\text{--}35$ MeV are shown in Figs. 1(b) and (c), respectively. These spectra show that excitation in the first energy range decays to a peak at about 20 MeV in the missing energy and that excitation in the second energy range decays to two peaks at about 20 and 26 MeV, which correspond to the 4.5- and 10.5-MeV excited states, respectively. This indicates that neutrons from the tail

region of the giant resonance in ^{40}Ca decay primarily to excited states of the residual nuclei: ^{39}Ca . As the excitation energy of ^{40}Ca increases, neutrons decay to higher excited states in ^{39}Ca , corresponding to excitation of deeper hole states. This result is very different from the neutron decay from the peak region of the giant resonance in ^{40}Ca [5]. Therefore, we have compared the missing energy spectra of the peak and tail regions of the giant resonance observed in the $(e, e'n)$ reaction in the p and $s\text{--}d$ shell nuclei in Fig. 2. In ^{12}C [1], the neutrons from the peak region ($\omega = 22.0\text{--}26.0$ MeV) of the giant resonance decay primarily to the ground state, and those from the tail region ($\omega = 42.5\text{--}47.5$ MeV) decay mainly to the ground state as well. Neutron decay to the excited states is small. In ^{28}Si [4], for the $s\text{--}d$ shell nuclei, neutrons from the peak region ($\omega = 20.5\text{--}28.5$ MeV) decay to the ground state (and the 1st and 2nd excited states). Conversely, the neutrons from the tail region ($\omega = 28.5\text{--}40.5$ MeV) decay to states higher than the ground state by about 5 MeV with a strength comparable to that observed for the ground state. In ^{40}Ca , the neutrons from the peak region ($\omega = 17\text{--}28$ MeV) decay to the ground and the first excited states (plus second and third excited states) [5], but neutrons from the tail region decay primarily to excited states at about 4.5 MeV and more. These experimental results show that in all cases, neutrons from the peak region decay to the ground and/or nearby states, whereas neutrons from the tail region decay to the ground state, the ground and excited states, or only to excited states depending on the nucleus.

To elucidate the nature of these neutron transitions to the excited state, the missing energy spectrum in the tail region was compared with the missing energy spectrum for quasielastic scattering in the $(e, e'p)$ reaction in Fig. 3 as exact information on the hole states has been obtained from quasielastic scattering in $(e, e'p)$. The missing energy spectra for the $(e, e'p)$ reaction with ^{28}Si and ^{40}Ca were measured at Saclay by Mougey *et al.* [9]. The range of the recoil momentum in Figs. 3(b) and (d) is $60 \leq P \leq 108$ MeV/c. In the figure, the abscissa is the excitation energy of the residual nucleus $E_x = E_m - E_{\text{th}}$, where E_m and E_{th} are the missing energy and the threshold energy of the reaction, respectively. The $^{28}\text{Si}(e, e'p)$ and $^{28}\text{Si}(e, e'n)$ spectra are very similar. In $^{28}\text{Si}(e, e'p)$ the first peak corresponds to the ground-state transition, where the protons were confirmed to be mainly $1d$ protons from the surface of the ^{28}Si nucleus, as shown by their momentum distributions. The second peak was interpreted as being because of the excitation of the $1p$ and $1s$ hole states. As the energy of the second peak in $(e, e'n)$ is consistent with the one in $(e, e'p)$, this second peak could be interpreted as being because of the neutrons from the $1p$ and $1s$ states in the ^{16}O core, that is, core excitation. As well, the $^{40}\text{Ca}(e, e'n)$ spectrum is compared with that of $^{40}\text{Ca}(e, e'p)$ in Figs. 3(c) and (d). In the $^{40}\text{Ca}(e, e'p)$ spectrum, four peaks centered at approximately 0, 3, 6, and 9 MeV can be seen. The shells were assigned to the $1d_{3/2}$, $2s$, and $1d_{5/2}$ states for the ground state, 3 MeV, and 6- and 9-MeV states, respectively [9]. For the state at about 3 MeV, contributions because of excitation from $1f_{7/2}$ and $2p_{3/2}$ states above the Fermi level in addition to core excitation have been observed in high-resolution $(e, e'p)$ experiments at NIKHEF [10]. Conversely, in the $^{40}\text{Ca}(e, e'n)$ spectrum two peaks centered at about 5 and 11 MeV can

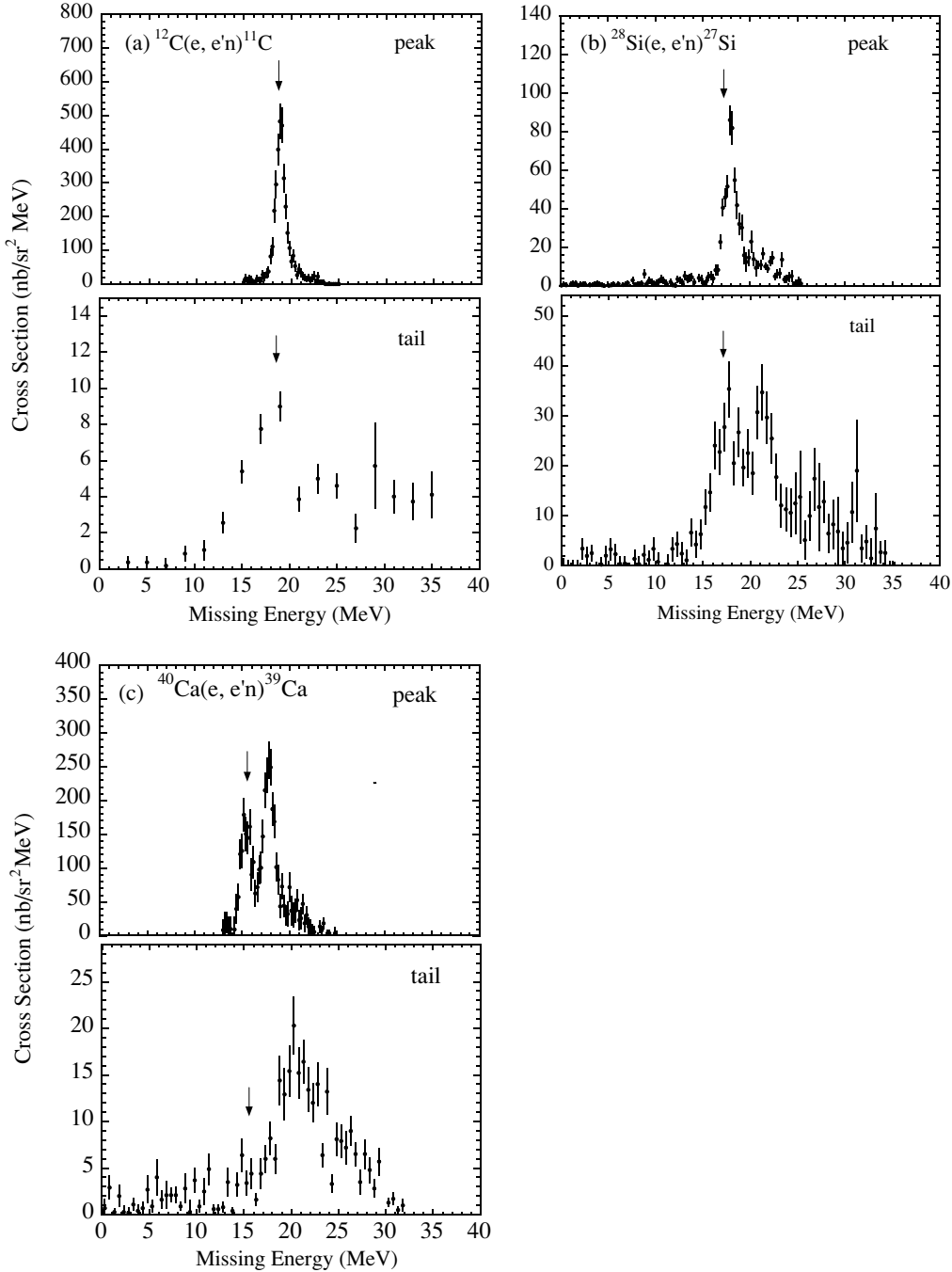


FIG. 2. Comparison between the missing energy spectra of the peak and the tail regions of the giant resonance observed in the $(e, e'n)$ reactions on ^{12}C (Ref. [1]), ^{28}Si (Ref. [4]), and ^{40}Ca . Arrows indicate the position of the ground-state transitions.

be seen. Comparing them with $(e, e'p)$ results, these peaks are considered to be because of the $2s_{1/2}$ and $1d_{5/2}$ neutrons although their energies do not agree with $(e, e'p)$ accurately. The neutrons from the tail in the $^{40}\text{Ca}(e, e'n)$ reaction do not decay to the ground state of the residual nuclei but decay to the excited states, corresponding to core excitation. This suggests that after core excitation, low-energy neutrons are easily emitted if the excitation energy is sufficient to excite the core, rather than high-energy neutrons with an energy nearly concentrated on one nucleon like in n_0 decay. The core

excitation reflects the nuclear shell structure as seen in the case of ^{12}C , ^{28}Si , and ^{40}Ca .

To confirm whether the tail region in the $(e, e'n)$ reaction is a part of the GDR, the angular correlations and cross sections for the $^{40}\text{Ca}(e, e'n)$ reaction have been measured in the excitation energy range extending from $\omega = 28$ to 35 MeV. The theoretical $(e, e'x)$ cross sections can be expressed as [11,12]:

$$d^3\sigma/d\Omega_e d\omega d\Omega_n = \sigma_M \{ V_L W_L + V_T W_T + V_{LT} W_{LT} \cos \phi_n + V_{TT} W_{TT} \cos 2\phi_n \}, \quad (1)$$

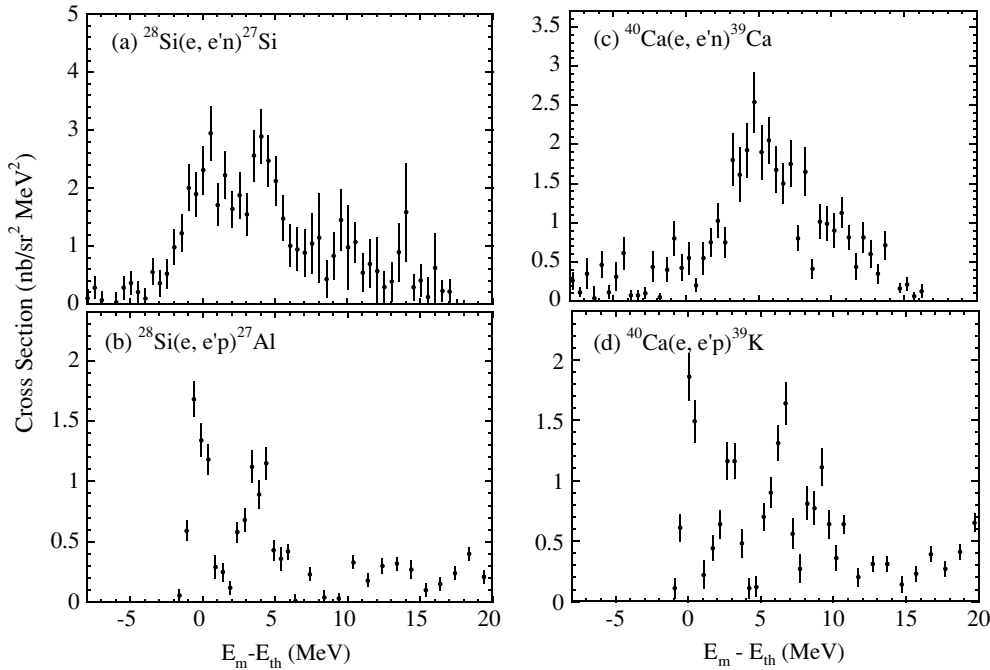


FIG. 3. Comparison between the missing energy spectra of the $(e, e'n)$ reaction and $(e, e'p)$ quasifree scattering (Ref. [9]) in ^{28}Si and ^{40}Ca . The range of the recoil momentum in $(e, e'p)$ is $60 \leq P \leq 108$ MeV/c. The horizontal scale is $E_m - E_{th}$.

where σ_M is the Mott cross section for scattering on a point nucleus and V_i are the leptonic kinematic factors. The structure functions W_i contain all the nuclear structure information. Under the present experimental conditions of forward scattering ($\theta_e = 30^\circ$), $q_{\text{eff}} = 0.35$ fm $^{-1}$, the giant dipole resonance is mainly excited through longitudinal interaction (C1); the transverse component (T1) and other multipoles (C2) may be weakly excited [13]. In this case, the longitudinal and transverse structure functions W_L and W_T can be expressed by $|C1|^2$, $C1^*C2$, and $|T1|^2$. The interference terms W_{LT} can be expressed by $C1^*T1$ and $C2^*T1$, and W_{TT} by $|T1|^2$. The present structure functions are approximated by Legendre polynomials up to the third order as follows:

$$\begin{aligned} V_L W_L + V_T W_T &= A_0[1 + b_1 P_1(x_n) + b_2 P_2(x_n) + b_3 P_3(x_n)], \\ V_{LT} W_{LT} &= C_2[c_1 P_1^1(x_n) + P_2^1(x_n) + c_3 P_3^1(x_n)], \\ V_{TT} W_{TT} &= D_2 P_2^2(x_n), \\ x_n &= \cos \theta_n. \end{aligned} \quad (2)$$

The $V_{TT} W_{TT}$ term was neglected in this analysis, because $V_{TT} W_{TT}$ is smaller than $V_T W_T$ in general [14,15]. The interference terms $c_1 P_1^1(x_n)$ and $c_3 P_3^1(x_n)$ were also neglected. These terms are assumed to be less than the main longitudinal-transverse interference term $C_2 P_2^1(x_n)$, because they involve interference between $E1$ and $E2$ in the longitudinal and transverse excitation modes. Five parameters, A_0 , b_1 , b_2 , b_3 , and C_2 , were used in the fitting, and these are shown in Figs. 4 and 5.

The cross section ($4\pi A_0$) is compared with the previous $(e, e'n)$ cross section measured in the peak region of the GDR [5] and (γ, n) results [16,17] in Fig. 4. The (γ, n) cross section in the peak region of the GDR was measured by Veyssière

et al. [16] and that in the tail region was measured by Murakami *et al.* [17]. These (γ, n) cross sections have been transformed into form factors with the usual method [5] and are compared with one another in the figure. The shape of the present $(e, e'n)$ cross section for the tail region seems to be roughly connected with the shape of the $(e, e'n)$ cross section for the peak region. The $(e, e'n)$ cross section is slightly larger than that of (γ, n) , but both $(e, e'n)$ and (γ, n) cross sections are very similar in

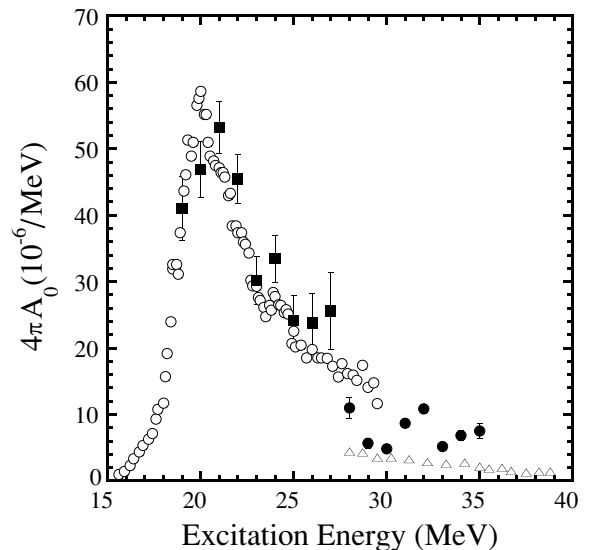


FIG. 4. Comparison of the present $^{40}\text{Ca}(e, e'n)$ cross section (closed circles) with the previous $(e, e'n)$ one (closed squares) from Ref. [5] and (γ, n) data from Ref. [16] (open circles) and Ref. [17] (open triangles).

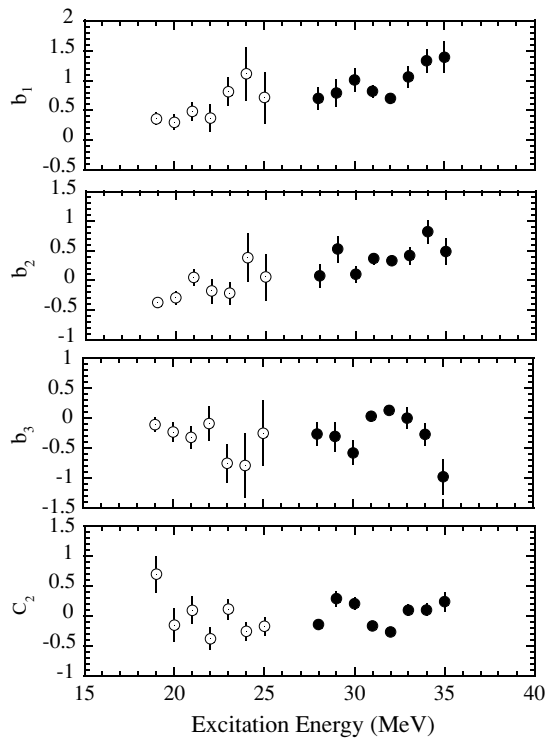


FIG. 5. Present $^{40}\text{Ca}(e, e'n)$ angular coefficients (closed circles) for the tail region of the GDR and previous $(e, e'n)$ data (open circles) for the peak region from Ref. [5].

shape. We conclude therefore that the present $(e, e'n)$ cross section just above the peak of the GDR may be regarded as the tail of the GDR.

The angular correlations of the tail region in the $^{40}\text{Ca}(e, e'n)$ reaction show a strong forward-backward asymmetry similar to those of the peak region of the GDR, which is different

from the angular correlation with a forward peak predicted from two-step processes like $(e, e'p)(p, n)$. The $^{40}\text{Ca}(e, e'n)$ angular coefficients for the tail region of the GDR together with those for the peak region are shown in Fig. 5. The b_i parameters correspond to E1, E2, and their interference components. If we compare the values of the b_1, b_2 , and b_3 around 21 and 29 MeV, which correspond to the positions of the peak and tail of the GDR, we observe that they are roughly identical for each parameter and these values are +0.5, 0, and -0.3 for b_1, b_2 , and b_3 , respectively. Similarly, the longitudinal-transverse interference parameter C_2 has a value roughly equal to zero in both regions. Thus, angular correlation results suggest as well that neutrons observed in the present measurements are because of the GDR.

In summary, we have measured the angular correlations and cross sections for the $^{40}\text{Ca}(e, e'n)$ reaction in the continuum above the giant resonance at a momentum transfer of 0.35 fm^{-1} . Comparing angular correlations and cross sections from the peak and tail regions of the GDR leads to the conclusion that neutrons emitted from the continuum are because of the tail of the GDR. A comparison of the missing energy spectra between the peak and the tail of the GDR indicates that neutron emission from the peak leads to populating the ground and first excited states, whereas neutron emission from the tail leads to excited states with an excitation energy higher than about 4.5 MeV. A comparison with $^{40}\text{Ca}(e, e'p)$ suggests that the latter is because of the $2s_{1/2}$ and $1d_{5/2}$ hole excitation (i.e., core excitation). The same situation was found in the $^{28}\text{Si}(e, e'n)$ reaction in the s - d shell nuclei but the situation is not clear in the $^{12}\text{C}(e, e'n)$ reaction of the $1p$ shell nuclei. The contribution of core excitation seems to increase with the mass number.

We thank the linac crew of the Laboratory of Nuclear Science for providing the quality beam.

-
- [1] K. Takahisa, T. Saito, S. Suzuki, C. Takakuwa, M. Oikawa, T. Nakagawa, T. Tohei, and K. Abe, Phys. Rev. C **66**, 014605 (2002).
- [2] T. Tadokoro, T. Hotta, T. Miura, M. Sugawara, A. Takahashi, T. Tamae, E. Tanaka, H. Miyase, and H. Tsubota, Nucl. Phys. **A575**, 333 (1994).
- [3] J. Ryckebusch, K. Heyde, D. van Neck, and M. Waroquier, Nucl. Phys. **A503**, 694 (1989), private communication.
- [4] K. Kino, T. Saito, T. Nakagawa, T. Nakagawa, and H. Ueno, Res. Rep. Nucl. Sci. Tohoku Univ. **33**, 1 (2000); **35**, 1 (2002).
- [5] C. Takakuwa, T. Saito, S. Suzuki, K. Takahisa, T. Tohei, T. Nakagawa, and K. Abe, Phys. Rev. C **50**, 845 (1994).
- [6] S. Strauch, P. von Neumann-Cosel, C. Rangacharyulu, A. Richter, G. Schrieder, K. Schweda, and J. Wambach, Phys. Rev. Lett. **85**, 2913 (2000).
- [7] T. Tamae *et al.*, Nucl. Instrum. Methods Phys. Res., Sect. A **264**, 173 (1988).
- [8] S. Suzuki, T. Saito, K. Takahisa, C. Takakuwa, T. Tohei, T. Nakagawa, Y. Kobayashi, and K. Abe, Nucl. Instrum. Methods Phys. Res., Sect. A **314**, 547 (1992).
- [9] J. Mougey, M. Bernheim, A. Bussière, A. Gillebert, Phan Xuan Hô, M. Priou, D. Royer, I. Sick, and G. J. Wagner, Nucl. Phys. **A262**, 461 (1976).
- [10] G. J. Kramer *et al.*, Phys. Lett. **B227**, 199 (1989).
- [11] M. Cavinato, D. Drechsel, E. Fein, M. Marangoni, and A. M. Saruis, Nucl. Phys. **A444**, 13 (1985).
- [12] T. de Forest, Ann. Phys. **45**, 365 (1967).
- [13] Y. Torizuka, K. Itoh, Y. M. Shin, Y. Kawazoe, H. Matsuzaki, and G. Takeda, Phys. Rev. C **11**, 1174 (1975).
- [14] W. E. Kleppinger and J. D. Walecka, Ann. Phys. (NY) **146**, 349 (1983).
- [15] G. Co' and S. Krewald, Nucl. Phys. **A433**, 392 (1985).
- [16] A. Veysière, H. Beil, R. Bergère, P. Carlos, A. Leprêtre, and A. de Miniac, Nucl. Phys. **A227**, 513 (1974).
- [17] T. Murakami *et al.*, J. Phys. G **14**, S275 (1988).